

Reinforced concrete wall as protection against accidental explosions in the petrochemical industry

Daniel Ambrosini[†]

*National University of Cuyo, CONICET, Argentina
Los Franceses 1537. 5600 San Rafael, Mendoza, Argentina*

Bibiana María Luccioni[‡]

*Structures Institute, National University of Tucumán, CONICET, Argentina
Country Las Yungas. 4107 Yerba Buena, Tucumán, Argentina*

(Received November 21, 2008, Accepted February 20, 2009)

Abstract. In this paper the study of a reinforced concrete wall used as protection against accidental explosions in the petrochemical industry is presented. Many alternatives of accidental scenarios and sizes of the wall are analyzed and discussed. Two main types of events are considered, both related to vessel bursts: Pressure vessel bursts and BLEVE. The liberated energy from the explosion was calculated following procedures firmly established in the practice and the effects over the structures and the reinforced concrete wall were calculated by using a CFD tool. The results obtained show that the designed wall reduces the values of the peak overpressure and impulse and, as a result, the damage levels to be expected. It was also proved that a reinforced concrete wall can withstand the blast load for the considered events and levels of pressure and impulse, with minor damage and protect the buildings.

Keywords: blast load; reinforced concrete; structural collapse; numerical analysis.

1. Introduction

Blasting loads have come to be forefront of attention in recent years due to a number of accidental and intentional events that affected important structures all over the world, clearly indicating that this issue is important for purposes of structural design and reliability analysis. As a result, extensive research activities in the field of blast loads have taken place in the last few decades.

Dynamic loads due to explosions result in strain rates of the order of 10^{-1} to 10^3 s^{-1} which implies short time dynamic behaviour of the materials involved, characterised mainly by a great overstrength and increased stiffness, in comparison with normal, static properties. In the case of concrete, the response is particularly complex due to the usual anisotropy and non linear nature of the material, and to the variability of mechanical properties. Normally, simplifying assumptions

[†] Dr. Eng., Professor, Corresponding author, E-mail: dambrosini@uncu.edu.ar

[‡] Dr. Eng., Professor, E-mail: bluccioni@herrera.unt.edu.ar

must be made in order to solve specific problems.

A blast wave originated in a closed or free explosive detonation behaves as a short duration dynamic load, when interacting with structures. Several studies have shown that such loads, with short duration and high magnitude, significantly influence the response of the structure and can substantially modify the expected material behaviour (Malvar *et al.* 1997, Dubé and Pijudier-Cabot 1996, Sercombe *et al.* 1998).

Plenty of research has been carried out concerning the behaviour of structural elements and materials under blast loads. Experimental results about the behaviour of steel (Jacinto *et al.* 2001), concrete (Yi 1991, Mays *et al.* 1999), fibre reinforced (Lok and Xiao 1999) panels and other composite materials (Tekalur *et al.* 2008) subjected to blast loads can be found in References. Recently, Buchan and Chen (2007) presented a state-of-the-art review about the experimental and finite element (FE) research in retrofitting concrete and masonry structures with fibre reinforced polymer (FRP) composites for blast protection.

In the literature, beams, slabs and shells under blast loads are mostly studied with limit analysis theory which assumes a rigid-plastic behaviour for the material (Yi 1991, Lubliner 1990). Yi (1991) tested concrete slabs under blast loads and studied the behaviour using a non-linear dynamic analysis. For close- in explosions the problem was solved with an approximate procedure. First, the zone just below the load is checked up on desintegration. If it has disintegrated, the level of damage is estimated. The tension failure of the other side of the plate is also studied with the aid of elastic theory. For the assessment of the dynamic displacement of the plate centre, a one degree of freedom model is used.

On the other hand, with the high development of computer hardware over the last decades, it has become possible to make detailed numerical simulations of the effects of blast loads on structures, significantly increasing the availability of these methods (Luccioni *et al.* 2004, Wu *et al.* 2005, Lu and Wang 2006).

Although there are still many uncertainties, material behaviour under blast loads has been widely studied experimentally (Brara *et al.* 2001, Le Nard *et al.* 2000, Cadoni *et al.* 2000) and many sophisticated numerical models have been proposed, especially for steel and concrete (Malvar *et al.* 1997, Zheng *et al.* 1999, Gebbeken and Ruppert 2000, Gatuingt and Pijudier-Cabot 2002, Lu and Xu 2004). The behaviour of concrete under blast loads is characterized by a different response in tension and compression, the progressive degradation of elastic properties accompanied by increasing permanent strains and the dependence of the strength, stiffness and fracture energy on strain rate. This last feature has been normally taken into account through viscoplastic models or rate-dependent damage models (Malvar *et al.* 1997, Dubé and Pijudier-Cabot 1996, Sercombe *et al.* 1998). These models have been included in different computer programs (Malvar *et al.* 1997, Gebbeken and Ruppert 2000, Gatuingt and Pijudier-Cabot 2000), which can be used for the analysis of the blast behaviour of structural elements and small structures and validated with available experimental results.

In this work the study of a reinforced concrete wall used as protection against accidental explosions in the petrochemical industry is presented. Many alternatives of accidental scenarios and sizes of the wall are analyzed and discussed.



Fig. 1 Layout of a typical plant and zone to be protected

2. Case study

2.1 Introduction

Since many accidents have taken place in the chemical industries all over the world, e.g., Flixborough, Seveso, Bhopal and recently at BP refinery in Texas City (U.S. Chemical Safety and Hazard Investigation Board 2007); the effects of this type of abnormal events need to be considered in order to lower the risk of people and building in the vicinities of the plants.

An incident database, involving oil, chemical, and biological discharges into the environment in the USA and its territories, is maintained by the National Response Center (NRC). In order to record accidents, European industries submit their data to the Major Accident-Reporting System (MARS) (Meel *et al.* 2007).

In this paper, the study and analysis of a reinforced concrete wall used as protection against accidental explosions in the petrochemical industry is presented. A view of a typical plant is shown in Fig. 1.

2.2 Events considered

In this paper two main types of events are considered, both related to vessel bursts: Pressure vessel bursts and BLEVE.

Pressure vessel bursts concern vessels containing a pressurised gas or vapour. The only source of energy for blast and fragmentation is the expansion of the gas or vapour. The liquid does not flash or it only slowly flashes, so that it will not supply a significant amount of energy. There is not fundamental difference in behaviour between vessels filled with ideal or non-ideal gases (TNO CPR 14E, 2005). In the case study, the pressure vessel burst of a propane compressor was considered.

A BLEVE (Boiling Liquid Expanding Vapor Explosion) is an explosion resulting from the failure of a vessel containing a liquid at a temperature significantly above its boiling point at normal atmospheric pressure, e.g., pressure liquefied gases. The fluid in the vessel is usually a combination of liquid and vapour. If the vessel ruptures, vapour is vented and the pressure in the liquid drops sharply. Upon loss of equilibrium, liquid flashes at the liquid-vapour interface, the liquid-container-

wall interface, and, depending on temperature, throughout the liquid. Instantaneous boiling throughout the liquid will occur whenever the temperature of the liquid is higher than the superheat temperature. A large fraction of the liquid can vaporize within milliseconds, liberating a very high amount of energy causing high blast pressures (TNO CPR 14E, 2005). In the case study the BLEVE of a Slug Catcher was considered.

For gas explosions different calculation methods exist and they are reviewed by Razuš and Krause (2001) and Ledin and Lea (2002). The BLEVE phenomena and its associated overpressures have been studied by means of analytical and numerical methods (van den Berg *et al.* 2004, Planas-Cuchi *et al.* 2004, Genova *et al.* 2008) as well as tests (Stawczyk 2003, Birk *et al.* 2007). Various recent real accidents involving BLEVE are described by Planas-Cuchi *et al.* (2004b), Park *et al.* (2006), U.S. Chemical Safety and Hazard Investigation Board (2007) and Bubbico and Marchini (2008).

2.3 Protection alternatives

In order to protect the inhabited buildings against the blast waves, a continuous wall was considered. A schematic design of the wall is shown in Fig. 2.

As design variables, the height of the wall and its distance to the inhabited buildings were selected (Fig. 3). Two alternatives for each case were analyzed, which are summarized in Table 1.



Fig. 2 Wall scheme

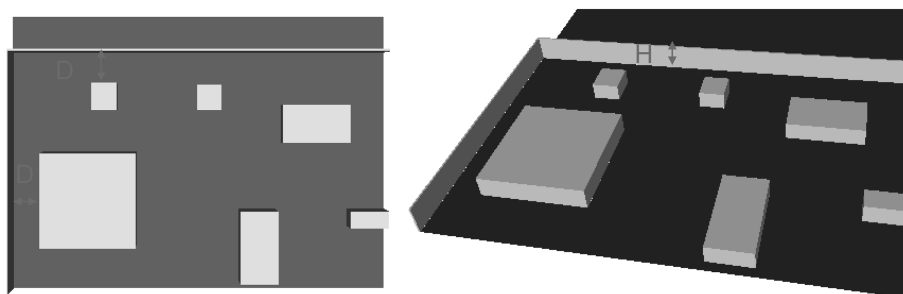


Fig. 3 Design variables analyzed

Table 1 Alternatives analyzed

Wall	D [m]	H [m]
W1	10	6
W2	10	8
W3	6	6

3. Action modelling

3.1 Introduction

A vessel rupture is coupled with the release of the contents and the release of the internal energy. Depending on the characteristics of the material in the vessel, the released contents can cause a buoyant fireball, a vapor cloud explosion, a flash fire or toxic gases. The sudden release of energy can give rise to damaging blast waves and high velocity fragments.

The calculation of blast and fragmentation effects can roughly be divided into two steps. In the first step the available energy is calculated, in the second step the effects are based on the energy resulting from the first step. This second step is basically the same for all types of vessel bursts. In the first step, however, distinction must be made between various types of vessel bursts. Different methods must be used for each way in which the internal energy can be liberated for transformation into mechanical energy. (TNO CPR 14E, 2005)

As it was mentioned in 2.2, pressure vessel bursts of a propane compressor and BLEVE of a slug catcher were considered in this paper.

The available energy (first step) is calculated following the procedures established in the TNO CPR 14E (Yellow Book) (2005) and the effects over the structures and the reinforced concrete wall (second step) are calculated by using a CFD tool as described in section 4.

3.2 Event 1

The procedure established in the TNO CPR 14E (Yellow Book), Chapter 7 is followed. In the case study, we consider the pressure vessel bursts of a propane compressor with a net volume of 440 m³. The available energy E_{av} from a pressure vessel burst may be calculated as

$$E_{av} = \frac{(P_1 - P_a)V_g}{\gamma_1 - 1} \quad (1)$$

In which P_1 is the vessel's internal pressure (absolute) at failure, P_a is the ambient pressure, V_g is the volume of gas-filled part of the vessel and γ_1 is the ratio of specific heats of the gas. In the analyzed case:

P_1 = the design overpressure of the vessel is 20.74 kg/cm². Then

$P_1 = 20.74 \text{ kg/cm}^2 = (2.03 + 0.1) \text{ MPa} = 2.13 \text{ MPa}$

P_a = ambient pressure = 101,325 Pa

γ_1 = the ratio of specific heats of the propane = 1.13

V_g = volume of the compressor 100% filled with propane: 440 m³

Then, the available energy of the explosion is: $E_{av} = 6.87 \text{ GJ}$

Table 2 Thermodynamic data for propane

T_1 (K)	p_1 (MPa)	h_f (kJ/kg)	h_g (kJ/kg)	v_f (m ³ /kg)	v_g (m ³ /kg)	s_f (kJ/kgK)	s_g (kJ/kgK)
369.8	4.24	879.2	879.2	$4.566 \cdot 10^{-3}$	0.0046	5.330	5.330
230.9	0.1	421.27	849.19	$1.722 \cdot 10^{-3}$	0.419	3.8721	5.7256

Table 3 Thermodynamic data for methane

T_1 (K)	p_1 (MPa)	h_f (kJ/kg)	h_g (kJ/kg)	v_f (m ³ /kg)	v_g (m ³ /kg)	s_f (kJ/kgK)	s_g (kJ/kgK)
350	4.24		1286		0.0438		10.008
111.5	0.1	285.38	796.9	$2.366 \cdot 10^{-3}$	0.567	4.928	9.521

3.3 Event 2

The procedure established in the TNO CPR 14E (Yellow Book), Chapter 7, is used for the calculus. In the case study, the BLEVE of a Slug catcher (two vessels) containing 80% of liquefied propane and 20% of vapor of methane with a total volume of 180 m³ is considered.

The thermodynamic properties of propane and methane at the corresponding temperatures (Perry and Green 1984) are summarized in Tables 2 and 3.

In which h_f and h_g are the specific enthalpies of the saturated liquid and vapor respectively, v_f and v_g are the specific volumes of the saturated liquid and vapor respectively, s_f and s_g are the specific entropies of the saturated liquid and vapor respectively, 4.24 MPa is the vessel's internal pressure (absolute) at failure, 230.9 K and 111.5 K are the boiling temperatures at atmospheric pressure of the propane and methane respectively, 369.8 K is the critical temperature of the propane and 350 K is the temperature of the methane at failure (At this combination of temperature and pressure, the methane is in gaseous state).

The work done by an expanding fluid (i.e., a liquid or a vapor) is defined as the difference in internal energy u between the fluid's initial and final states. The internal energy at initial state may be calculated as

$$u_1 = h - Pv \quad (2)$$

In which h is the specific enthalpy (enthalpy per unit mass), P the absolute pressure and v the specific volume.

The thermodynamic properties of mixtures of fluids are usually not known. A crude estimate of a mixture internal energy can be made by summing up the internal energy of each component.

In this case, for liquid:

$$u_1 = 879.2 \cdot 10^3 - 4.242 \cdot 10^6 \times 4.566 \cdot 10^{-3} = 859.831 \text{ kJ/kg}$$

For vapor:

$$u_1 = 1286 \cdot 10^3 - 4.0 \cdot 10^6 \times 0.0438 = 1110.8 \text{ kJ/kg}$$

The specific internal energy in the expanded state u_2 can be determined assuming an isentropic expansion (entropy s constant) to atmospheric pressure. Then, the internal energy at final state may be calculated as

$$u_2 = (1 - X) h_f + X h_g - (1 - X) P_a v_f - X P_a v_g \quad (3)$$

In which X is the vapor ratio $= (s_1 - s_f)/(s_g - s_f)$ and s the specific entropy.

In this case, for liquid:

$$X = (5.33 - 3.8721)/(5.7256 - 3.8721) = 0.787$$

$$u_2 = (1 - 0.787) \times 421.27 \cdot 10^3 + 0.787 \times 849.19 \cdot 10^3 - (1 - 0.787) \times 0.1 \cdot 10^6 \times 1.722 \cdot 10^{-3} - 0.787 \times 0.1 \cdot 10^6 \times 0.419 = 724.896 \text{ kJ/kg}$$

For vapor:

$$X = (10.008 - 4.928)/(9.521 - 4.928) = 1.1 \cong 1$$

$$u_2 = 796.9 \cdot 10^3 - 0.1 \cdot 10^6 \times 0.567 = 740.2 \text{ kJ/kg}$$

The specific work e_{av} done for an expanding fluid is:

$$e_{av} = u_1 - u_2 \quad (4)$$

In this case, for liquid:

$$e_{av} = 859.831 - 724.896 = 134.94 \text{ kJ/kg}$$

For vapor:

$$e_{av} = 1110.8 - 740.2 = 370.6 \text{ kJ/kg}$$

The total masses of liquid M_l and vapor M_v are:

$$M_l = 0.80 \cdot 180 / (4.566 \cdot 10^{-3}) = 31,537 \text{ kg}$$

$$M_v = 0.20 \cdot 180 / 0.0438 = 822 \text{ kg}$$

Then, the explosion energy for the saturated liquid E_l and vapor E_v are:

$$E_l = 134.94 \cdot 10^{-3} \cdot 31,537 = 4,255.62 \text{ MJ}$$

$$E_v = 370.6 \cdot 10^{-3} \cdot 822 = 304.63 \text{ MJ}$$

Assuming that the blast of the expansion of the vapor is synchronous with the blast from the flashing of the liquid, the total energy of the surface explosion is:

$$E_{av} = 4.56 \text{ GJ}$$

3.4 TNT Equivalency

Considering the specific energy of the TNT and the total energy of the explosion, an equivalent mass of TNT could be obtained dividing both terms. However, it is recognised in the specialised literature that this method introduces a significant overestimation of the obtained overpressures (Planas-Cuchi *et al.* 2004, Birk *et al.* 2007).

Then, an ad-hoc procedure was used in order to obtain reliable TNT equivalencies: Following the procedure established in the TNO CPR 14E (Yellow Book), Chapter 7, the overpressures and

impulses at the location of the wall were determined for each event. Then, an equivalent TNT mass that produces the same shock overpressures and impulses was determined in each case. Finally, a hydrocode was used, incorporating the TNT mass obtained in the previous step, in order to take into account the multiple reflections of the shock wave and its results are presented in the following sections.

Then, the obtained TNT equivalencies are:

Event 1: 600 kg TNT

Event 2: 400 kg TNT

Although compared to a TNT-explosion, the shock wave produced by bursting vessels has lower initial overpressures, a slower decay of the overpressure with distance, longer positive phase durations, much larger negative phases and strong secondary shocks, it is recognized that the TNT-equivalence method gives reasonable results for far field (TNO CPR 14E, Yellow Book, 2005, Birk *et al.* 2007). However, the engineering approach presented in this point could be applied in the far as well as in the near field and the results, in terms of equivalent-mass of TNT, are comparable to those obtained by Planas-Cuchi *et al.* (2004) based on a more realistic assumption of irreversible adiabatic expansion. This important topic will be discussed in detail in another paper.

4. Numerical models

4.1 Introduction

Important effects such as multiple blast wave reflections, the Mach effect, rarefactions, and the negative phase of the blast wave can be readily modeled in computational fluid dynamics (CFD) codes. Simplified analytical and semiempirical techniques often ignore such phenomena. In this paper, the program AUTODYN-3D (2007), which is an “hydrocode” that uses finite difference, finite volume, and finite element techniques to solve a wide variety of non-linear problems in solid, fluid and gas dynamics, is used with these purposes.

Computer models used to simulate the propagation of the blast wave generated by the explosions considered and their action on buildings are described in this section.

One of the major problems associated with computer modeling of this type of problems that is referred to in most recent publications is the great calculus volume that makes it nearly impossible to solve the complete problem in existent computers with the mesh refinement required to achieve the accuracy needed (Børvik *et al.* 2008, Lu and Wang 2006, Luccioni *et al.* 2004). For this reason, different numerical models that cover the action and the building studied were developed for each accident scenario.

On the other side, it is well known that the pressure wave generated by the explosion presents axial symmetry until it reaches a medium different from air. So the problem can be initially solved in two dimensions with a dense mesh, until the pressure wave reaches the first obstacle. This was the procedure used in this paper. The first instants of the blast wave propagation were simulated in axial symmetric models with variable ratio and 50 m height. Air flow out was allowed in the upper surface while the lower surface was considered to be rigid representing the floor where the blast wave reflects, see Fig. 4.

Before the blast wave reaches any obstacle, the results of this first two dimensional analysis were

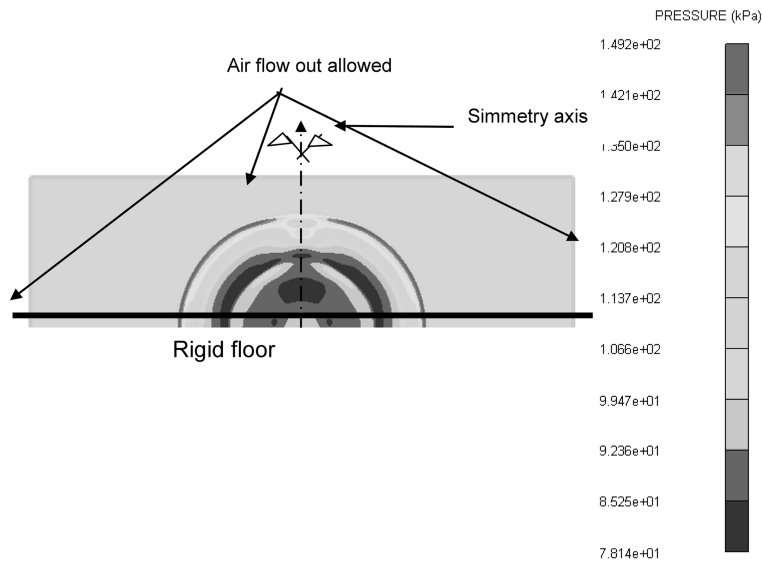


Fig. 4 Axial simmetric model. First instants of blast wave propagation

mapped on three dimensional models with coarser meshes. In this way, the computer time is substantially reduced and the analysis of wide problems like that analyzed in this paper, is possible.

An Euler processor was used for air in all the models, while walls and structures were supposed to be rigid in the first part of the analysis where the protection provided by the wall was assessed. It is well known that the peak reflected overpressure depends on the surface stiffness. Nevertheless, previous works of the same authors have demonstrated that the influence of masonry and concrete structures flexibility is negligible for the type of analysis performed in this paper (Luccioni *et al.* 2005, 2006).

Cubic cells of 500 mm side were used to model air in all the models presented. Previous work (Luccioni *et al.* 2006) and comparison with existent empirical equations (Smith and Hetherington 1994, Baker *et al.* 1983, Kinney and Graham 1985) for the assessment of side-on overpressures have shown that those dimensions are appropriate for the analysis of blast loads on buildings.

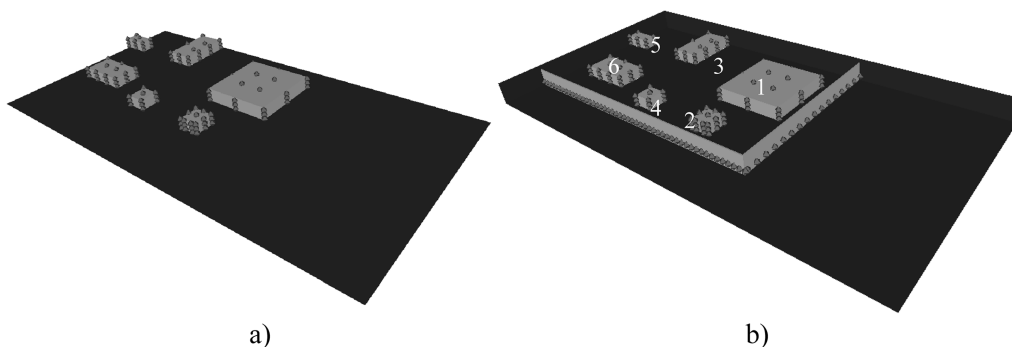


Fig. 5 Model for the pressure vessel bursts of a propane compressor. a) Without protection wall. b) With protection wall

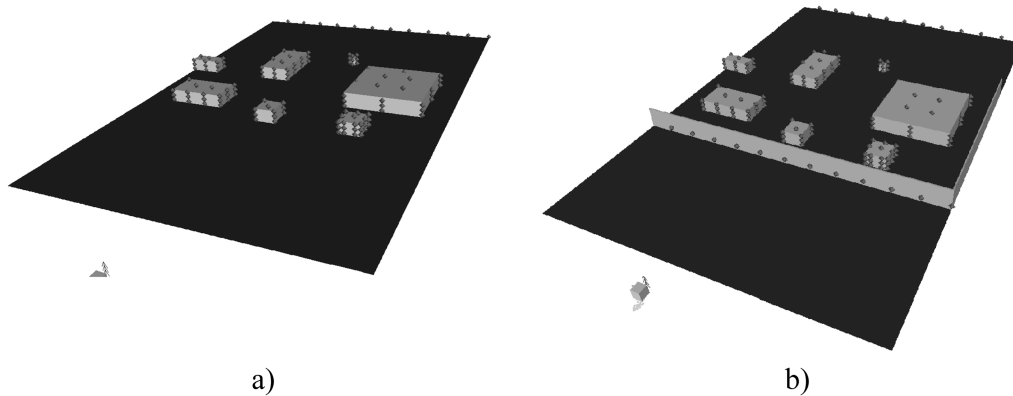


Fig. 6 Model for the BLEVE of a Slug Catcher. a) Without protection wall, b) With protection wall

Control points were located on all the models to record the pressure and impulse time history. The location of these points is illustrated in Figs. 5 and 6.

Fig. 5 shows the models used to simulate the effect of the pressure vessel burst of the propane compressor on buildings. Buildings are numbered in white. An air volume of $184 \text{ m} \times 81 \text{ m}$ and 10 m of height, with 1.413.120 cells was used. Air flow out was allowed in all sides of the model except for the bottom surface where a rigid surface representing the floor was considered. In Fig. 5(a) the situation without wall was considered while Fig. 5(b) corresponds to one of the protection walls modeled.

Fig. 6 represents the model used to simulate the load generated by the slug catcher BLEVE. An air volume of $240 \text{ m} \times 374 \text{ m}$ and 10 m height was modelled.

5. Numerical results

5.1 Wave propagation

The propagation of the blast wave generated by the pressure vessel burst of the propane compressor is presented in Fig. 7 where values of pressure reflected on the building and floor surfaces for different time instants are represented.

The different models were run on a PC-based computer with Core 2 Duo Processor of 2.2 GHz and 2 Gb of RAM Memory. The runtime of a typical example was approximately 8 hours.

It is clear that the blast wave that was originally spherical losses its symmetry when it reaches the buildings and makes it difficult the assessment of pressure values through empirical formulae.

In order to study the effect of the protection wall on the blast wave propagation, the same problem but with the different walls proposed was also analyzed. The pressure wave propagation for the case of protection wall W2 is illustrated in Fig. 8. The reflection of the blast wave on the wall and the protection on the buildings due to the presence of the wall are evident in Fig. 8.

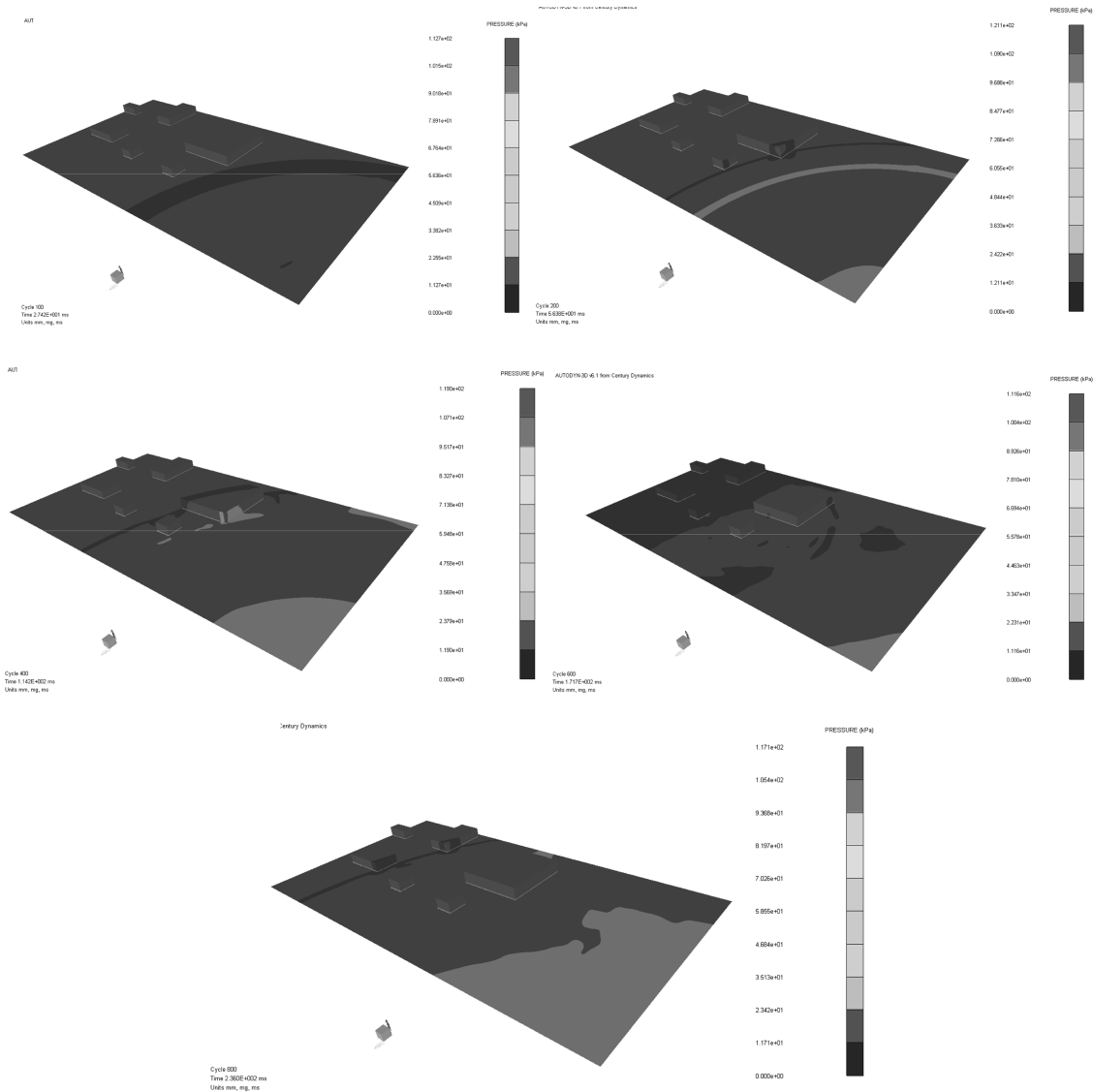


Fig. 7 Pressure vessel burst of the propane compressor. Blast wave propagation

5.2 Pressure time histories

When the shock wave produced by the explosion reaches a solid surface, an instantaneous change of pressure due to the reflection of the side on pressure and the action of the dynamic pressure or wind occurs. In general, the peak reflected pressure depends on the intensity of the incident wave, the angle of incidence and the nature of the reflecting surface.

The reflected pressure time histories on the buildings closest to the explosion are presented in the following figures for the different accidents considered. The curves corresponding to the cases without and with different walls are presented and compared. In all the cases the curves correspond

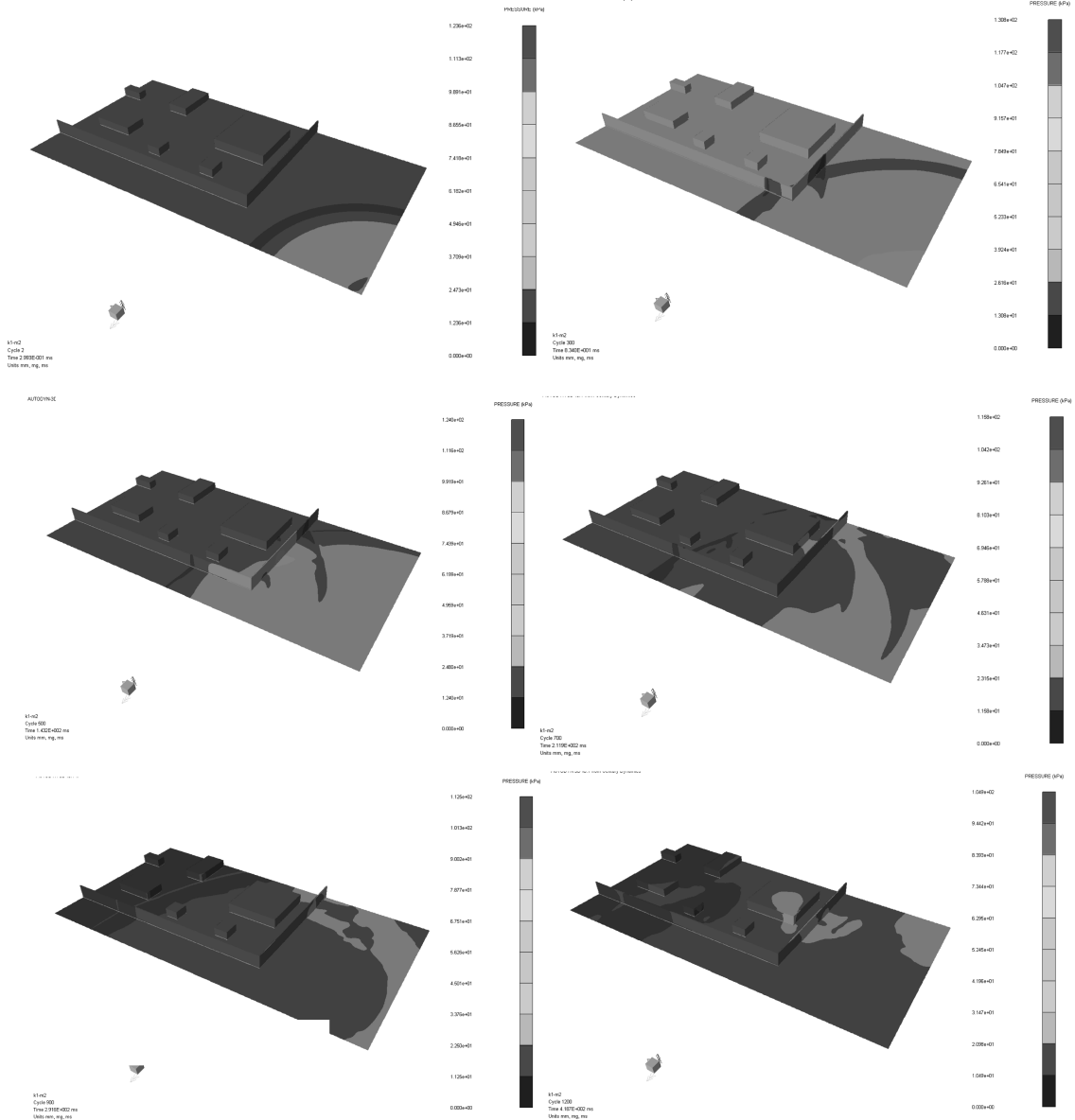


Fig. 8 Pressure vessel burst of the propane compressor. Blast wave propagation with protection wall W2

to the points with the greatest pressure value.

Fig. 9 shows the pressure time histories on building 1 produced by the pressure vessel burst of the propane compressor and the BLEVE of the slug catcher. It can be observed that all the protection walls studied reduce the value of the peak reflected overpressure. Nevertheless, the reduction of the peak reflected overpressure (one half) due to the protection wall W2 is greater than that produced by the other walls studied.

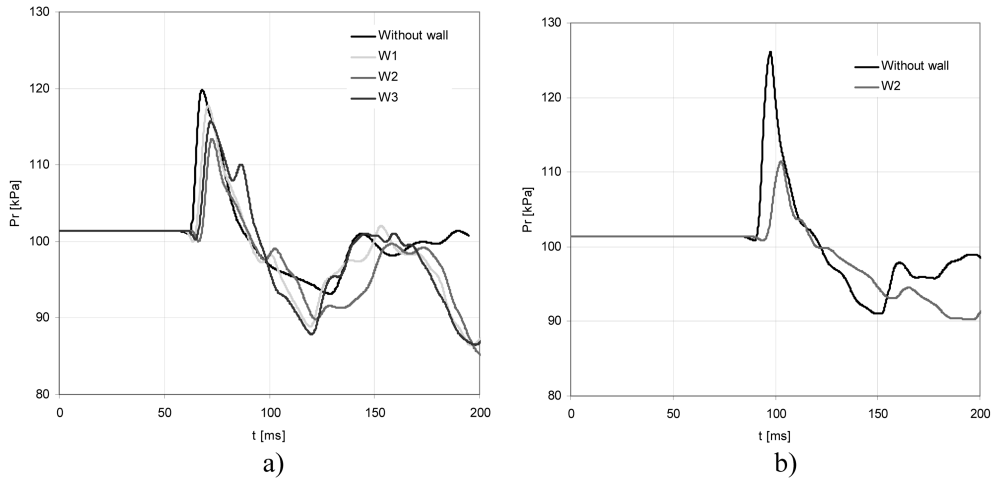


Fig. 9 Reflected pressure time histories on building 1. a) Pressure vessel burst of propane compressor, b) Slug catcher BLEVE

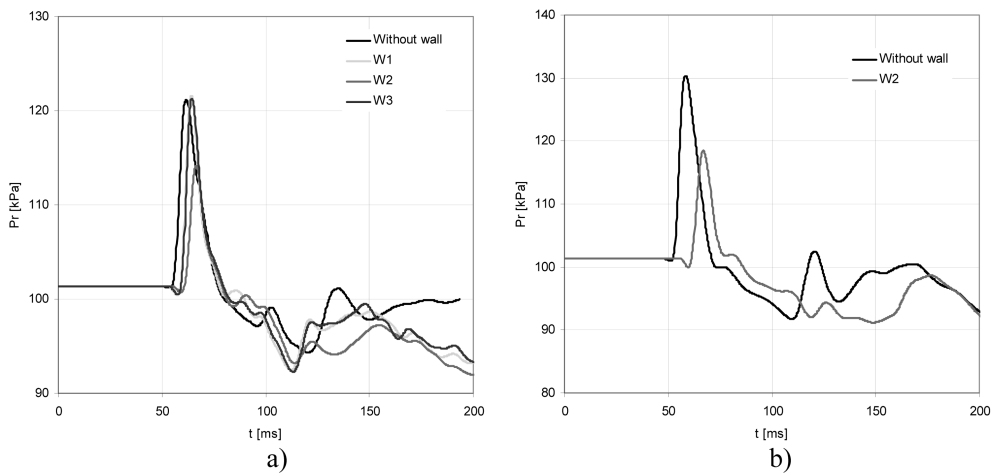


Fig. 10 Reflected pressure time histories on building 2. a) Pressure vessel burst of propane compressor, b) Slug catcher BLEVE

The reflected pressure time histories on building 2 are presented in Fig. 10. The values of the peak overpressure are similar to those of building 1. The protection walls reduce the peak pressure and delay the arriving of the pressure wave. The pressure reduction due to wall 2 is greater than that corresponding to the other walls.

5.3 Peak reflected pressure

A simple and common way of estimating the risk of structures exposed to blast loads is through the values of the maximum side on overpressure. The values of the side on peak overpressure in the zone of buildings due to the pressure vessel burst of the propane compressor and the BLEVE of the

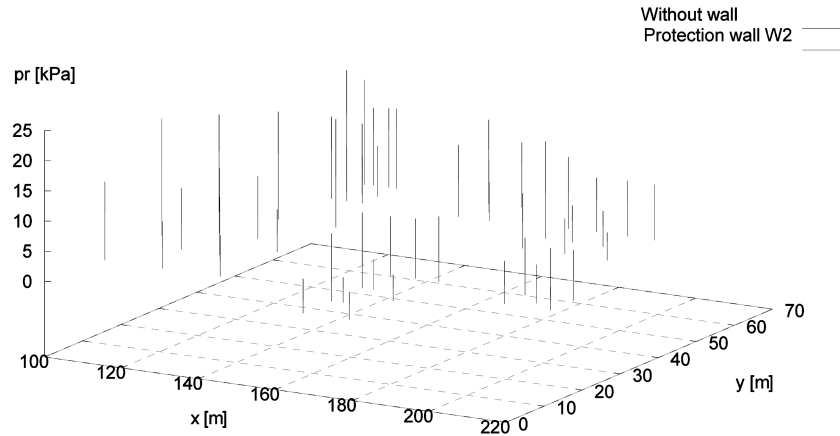


Fig. 11 Peak reflected overpressure due to pressure vessel burst of the propane compressor

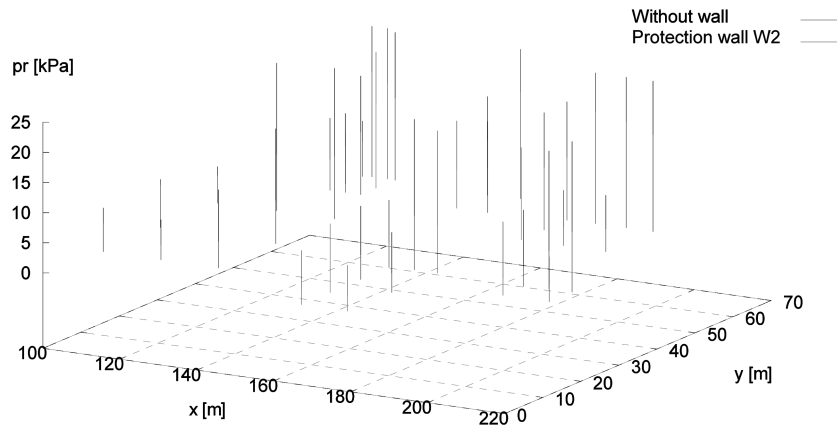


Fig. 12 Peak reflected overpressure due to the BLEVE of the Slug Catcher

slug catcher are plotted in Figs. 11 and 12 respectively, where the values obtained without wall and with protection wall W2 are compared. The pressure reduction provided by protection wall W2 is evident in both figures.

5.4 Damage assessment

The assessment of damage due to explosive-produced loads on structures can be performed with any numerical tool from the hydrocode type. However, this would require the detailed discretization of the buildings analysed and could be prohibitive in terms of time and cost in the case of a wide area with many buildings such as the one considered here. Alternatively, the use of isodamage curves, which can be found in the literature (Smith and Hetherington 1994, Baker *et al.* 1983, Elliot *et al.* 1994, Millington 1994) seems to be a more attractive way to relate pressures and impulses approximately to damage produced in different types of building and parts of them. In general, isodamage curves have been obtained from a wide compilation of data related to damage produced in masonry houses and other buildings and structural elements in both experimental and actual

explosions. One of the diagrams used in this paper is that one presented by Baker (Elliott *et al.* 1992, Baker *et al.* 1983, Smith and Hetherington 1994) that relates different damage levels in brick-built houses to peak reflected overpressure (P_r and impulse, i_r). The different damage levels defined correspond to:

- (a) Zone A (above line B): almost complete demolition;
- (b) Line B: such severe damage as to require demolition; 50-70% of external brickwork destroyed or unsafe;
- (c) Line Cb: damage rendering house temporarily uninhabitable; partial collapse of roof and one or two external walls; load-bearing partitions severely damaged, requiring replacement;
- (d) Line Ca: relatively minor structural damage, yet sufficient to make house temporarily uninhabitable; partitions and joinery wrenched from fixings
- (e) Zone D (below line Ca): damage calling for urgent repair, but not so as to make house uninhabitable; damage to ceilings and tiling; more than 10% of glazing broken.

These diagrams define global levels of damage to assess safety and need for demolition, but do not make precise reference to the type of wall or structure affected by the explosion. As an alternative, the diagrams presented by Millington (1994) which relate incident overpressure to distance for different masses of explosive and damage levels, were used. These curves correspond to masses of explosive from 1 to 500 kg of TNT, and have a finer specification for damage levels in different types of structural and non-structural elements.

Both types of isodamage diagrams must be converted into diagrams relating reflected pressures and impulses to damage levels in order to use them to obtain the levels of damage corresponding to reflected values of pressure and impulse obtained in the numerical simulation. The resulting curves, which are obtained by using empirical expressions and charts (Smith and Hetherington 1994, Baker *et al.* 1983, Elliot *et al.* 1994) are presented in Fig. 13 (Luccioni *et al.* 2005).

The results of the simulated pressure and impulses, obtained for the buildings faces and all the protection alternatives studied, are plotted on the isodamage diagrams in Figs. 14 and 15.

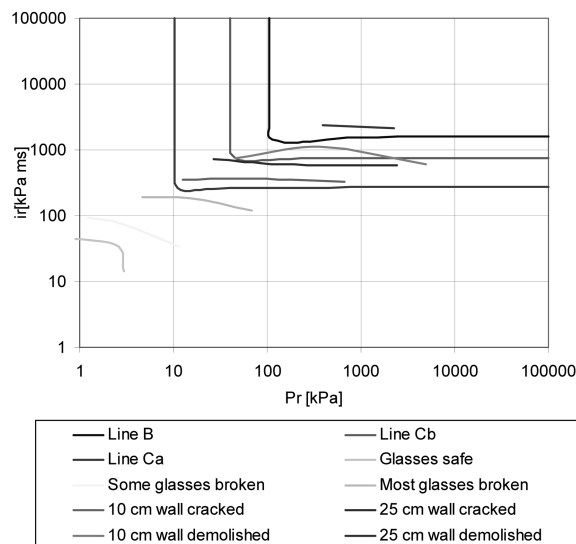


Fig. 13 Isodamage curves

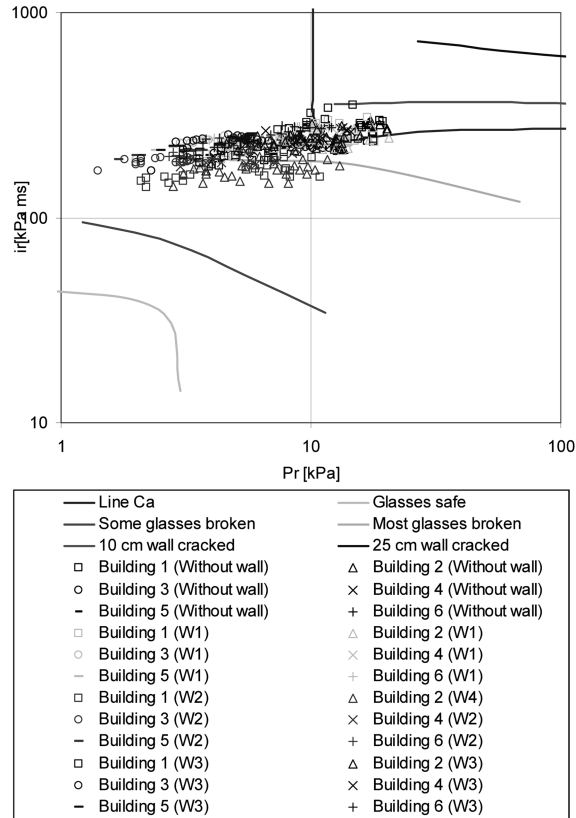


Fig. 14 Damage levels for the pressure vessel burst of the propane compressor

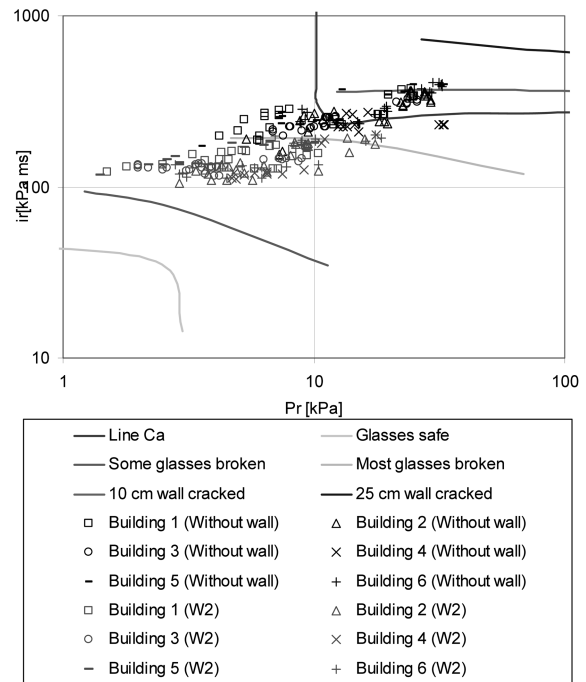


Fig. 15 Damage levels for the slug catcher BLEVE

It is important to note that the buildings studied are mainly masonry buildings like those for which the isodamage curves were obtained (Elliott *et al.* 1992, Baker *et al.* 1983, Smith and Hetherington 1994).

Damage levels for the different protection alternatives can be easily compared using Figs. 14 and 15. It is clear that buildings 1 and 2 are more exposed than the rest of the buildings for both accident scenarios analysed. A reduction of damage levels is achieved with protection walls W1 and W3 that protect most of the buildings except for building 1. Protection wall W2 that is scarcely higher than building 1 protects all the building reducing damage levels to the zone of broken glasses in the case of the pressure vessel burst of the propane compressor and to the zone of 10 cm thickness wall cracked in the case of the slug catcher BLEVE.

6. Reinforced concrete wall assessment

The protection provided by wall W2 was analysed in previous section. This reinforced concrete wall is now analyzed in order to prove if it is able to withstand pressures and impulses generated by the accident scenarios considered. The wall that was supposed to be rigid in previous section was modeled again but with its actual thickness and materials in this part of the work.

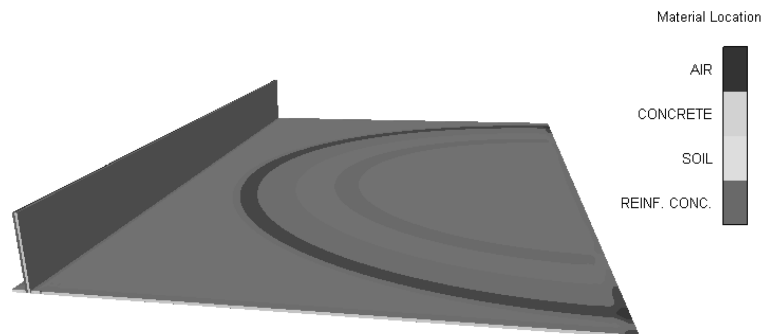


Fig. 16 Model used for damage assessment of the reinforced concrete protection wall W2

The model used for this analysis is shown in Fig. 16 that corresponds to the case of the slug catcher BLEVE. For this purpose, the air block comprising only the focus of the explosion and the wall was modeled with a 500 mm side cubic Euler FCT grid. It is important to note that the event slug catcher BLEVE produces the higher overpressures and impulses over the wall. In the case studied, the maximum pressure and impulse over the wall are 43 kPa and 560 kPa ms respectively.

A 500 mm thick wall was adopted based on a simple static analysis. The wall was modeled with a Lagrange processor and Euler-Lagrange meshes interaction was activated. The wall was fixed at its base and ends. A finer grid of 250 mm side was used for the wall.

An RHT model with the properties presented in Table 4 was used for concrete. This is a modular strength model for brittle materials that is particularly useful for modeling the dynamic loading of concrete. The model computes the following phenomena associated with brittle materials : pressure hardening, strain hardening, strain rate hardening, third invariant dependence for compressive and tensile meridians, damage effects (strain softening), volumetric compaction (using the P-alpha) and crack-softening.

Although reinforced concrete elements can be modeled as a combination of concrete and steel elements joined together with the assumption of perfect bond, this type of model is prohibited for actual structures, as it requires a great number of elements. Moreover, the time step in explicit dynamic programs is directly related to the size of the elements (Luccioni and Luege 2006). Taking into account the above considerations, an approximate material model was defined to simulate the behavior of reinforced concrete. A homogenized model similar to that of concrete but with higher stiffness and tension strength was used to consider the contribution of the reinforcement. The mechanical properties of the homogenized model used for reinforced concrete are also shown in Table 4. The back layer of the wall was filled with that material while the other layers (facing the blast load) were all filled with concrete with the same properties in Table 4.

In order to reproduce the fracture of the concrete wall, an erosion model was used to remove from the calculation the cells that have reached certain criteria based on deformations. This erosion model represents a numerical remedial measure to counteract the great distortion that can cause excessive deformation of the mesh. For this reason, its application to simulate a physical phenomenon requires calibration with experimental results. The erosion limit was calibrated according to experimental and empirical results (Luccioni and Luege 2006). An erosion limit of 0.1 of instantaneous geometrical strain was used.

As described in previous section the problem was first analyzed in two dimensions with an axial

Table 4 Concrete and reinforced concrete (in brackets) mechanical properties

Equation of State	P alpha	Strength	RHT Concrete
Reference density	2.75000E+00 (g/cm ³)	Shear Modulus	1.67000E+07 (kPa)
Porous density	2.31400E+00 (g/cm ³)	Compressive Strength (fc)	3.50000E+04 (kPa)
Initial compaction pressure	2.33000E+04 (kPa)	Shear Strength (fs/fc)	1.80000E-01
Solid compaction pressure	6.00000E+06 (kPa)	Intact Failure Surface Constant A	1.60000E+00
Compaction exponent	3.00000E+00 (none)	Intact Failure Surface Exponent N	6.10000E-01
Solid EOS	Polynomial	Tens./Comp. Meridian Ratio (Q)	6.80E-01 (8.00E-01)
Bulk Modulus A1	3.52700E+07 (kPa)	Brittle to Ductile Transition	1.05000E-02
Compaction Curve	Standard	Tensile Strain Rate Exp. Delta	3.60000E-02 (none)

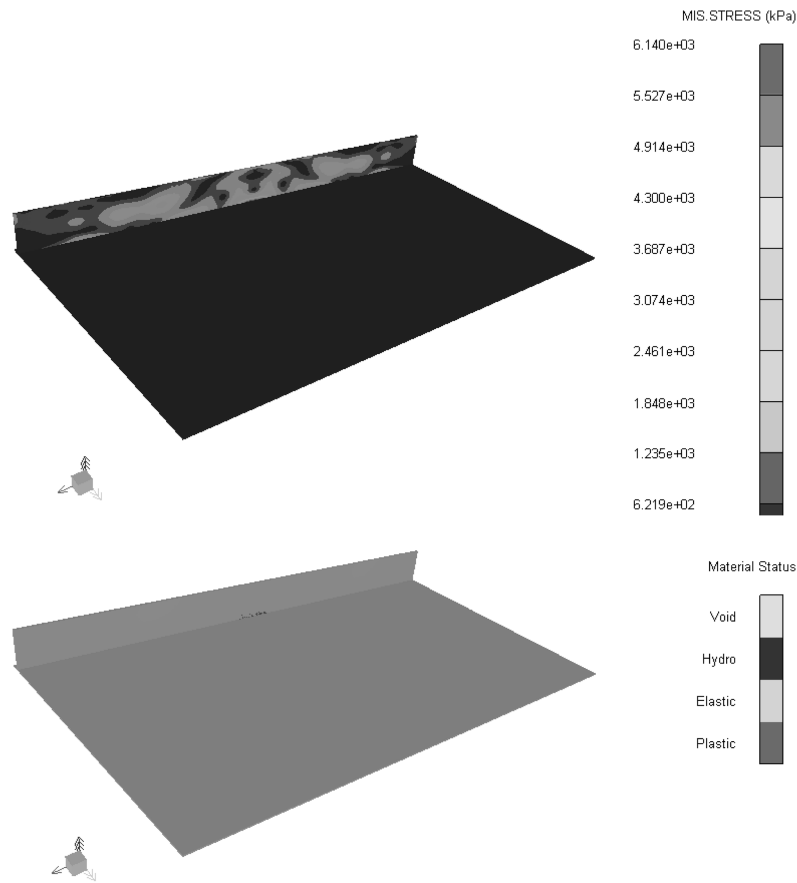


Fig. 17 Results for t = 0.3s: a) Von Mises stress b) Plastic zones

symmetric model. Before the blast wave reached the wall, the results were mapped on the three dimensional model to simulate the blast load action on the wall.

Figs. 17 shows the Von Mises stress on the wall and the plastic zones resulting after 0.3s. It is clear that there is only minor damage at the base of the wall indicating that it can withstand the

explosive wave and protect the buildings.

The same analysis with similar results was also performed for the pressure vessel burst of the propane compressor.

7. Conclusions

The results obtained show that the designed wall reduces the values of the peak overpressure and impulse and, as a result, the damage levels to be expected. It was also proved that a reinforced concrete wall can withstand the blast load for the considered events and levels of pressure and impulse, with minor damage and protect the buildings. For this reason, it is clear that the incorporation of an appropriated designed wall is an useful alternative to consider when it is necessary to reduce the risk levels associated to accidental explosions.

It is clear that the blast wave that is originally spherical losses its symmetry when it reaches the obstacles. This fact makes it difficult the assessment of pressure values through empirical formulae in environments with obstacles.

Moreover, the results obtained in this paper show that, within the zone studied, buildings 1 and 2 are the most exposed ones and therefore need some protection. Among the different protection alternatives analyzed, the wall of 8m height located at 10 m of the nearest buildings results to be more efficient. Walls closer to the buildings only protect the nearest buildings leaving the rest unprotected or even more exposed. Lower walls are not efficient enough. The height of the wall should be at least equal to that of the highest building to be protected.

The presence of this wall reduces the values of the peak overpressure and impulse and, as a result, the damage levels to be expected.

It was also proved that a reinforced concrete wall can withstand the blast load with minor damage and protect the buildings for the cases analyzed with the levels of pressures and impulses indicated in point 6.

Other protection alternatives comprising earth barriers close to the explosion and smaller reinforced concrete walls near the buildings should be analyzed.

Acknowledgements

The financial supports of the CONICET (Argentina), National University of Cuyo and National University of Tucumán are gratefully acknowledged. The authors also wish to thanks Ms. Amelia Campos for the English revision

References

- Baker, W.E., Cox, P.A., Westine, P.S., Kulesz, J.J. and Strehlow, R.A. (1983), *Explosion Hazards and Evaluation*. Amsterdam: Elsevier.
- Birk, A.M., Davison, C. and Cunningham, M. (2007), "Blast overpressures from medium scale BLEVE tests", *J. Loss Prevent. Proc.*, **20**, 194-206.
- Børvik, T., Hanssen, A.G., Langseth, M. and Olovsson, L. (2008), "Response of structures to planar blast loads -

- A finite element engineering approach”, *Comput. Struct.*, In press.
- Brara, A., Camborde, F., Klepaczko, J.R. and Mariotti, C. (2001), “Experimental and numerical study of concrete at high strain rates in tension”, *Mech. Mater.*, **33**, 33-45.
- Bubbico, R. and Marchini, M. (2008), “Assessment of an explosive LPG release accident: A case study”, *J. Hazardous Mater.*, **155**(3), 558-565.
- Buchan, P.A. and Chen, J.F. (2007), “Blast resistance of FRP composites and polymer strengthened concrete and masonry structures – A state-of-the-art review”, *Composites: Part B*, **38**, 509-522.
- Cadoni, E., Labibes, K., Berra, M., Giangrasso, M. and Albertini, C. (2000), “High-strain-rate tensile behaviour of concrete”, *Mag. Concrete Res.*, **52**(5), 365-370.
- Dubé, J.F. and Pijaudier-Cabot, G. (1996), “Rate-dependent damage model for concrete in dynamics”, *J. Eng. Mech.*, ASCE, **122**(10), 939-947.
- Elliott, C.L., Mays, G.C. and Smith, P.D. (1992), “The protection of buildings against terrorism and disorder”, *P. I. Civil Eng.- Str. B.*, **94**, 287-297.
- Gatuingt, F. and Pijaudier-Cabot, G. (2000), “Computational modelling of concrete structures subjected to explosion and perforation”, *Proceeding of Ecomass 2000*, Barcelona.
- Gatuingt, F. and Pijaudier-Cabot, G. (2002), “Coupled damage and plasticity modelling in transient dynamic analysis of concrete”, *Int. J. Numer. Anal. Meth. Geomech.*, **26**, 1-24.
- Gebbeken, N. and Ruppert, M. (2000), “A new material model for concrete in high-dynamic hydrocode simulations”, *Arch Appl. Mech.*, **70**, 463-478.
- Genova, B., Silvestrini, M. and Leon Trujillo, F.J. (2008), “Evaluation of the blast-wave overpressure and fragments initial velocity for a BLEVE event via empirical correlations derived by a simplified model of released energy”, *J. Loss Prevent. Proc.*, **21**, 110-117.
- Jacinto, A., Ambrosini, R.D. and Danesi, R.F. (2001), “Experimental and computational analysis of plates under air blast loading”, *Int. J. Impact Eng.*, **25**(10), 927-947.
- Kinney, G.F. and Graham, K.J. (1985), *Explosive Shocks in Air*. 2nd ed. Berlin: Springer Verlag.
- Le Nard, H. and Bailly, P. (2000), “Dynamic behaviour of concrete: the structural effects on compressive strength increase”, *Mech. Cohes-Frict Mater.*, **5**, 491-510.
- Ledin, H.S. and Lea, C.J. (2002), *A Review of the State-of-the-Art in Gas Explosion Modelling*. Report HSL/2002/02. Health and Safety Laboratory.
- Lok, T.S. and Xiao, J.R. (1999), “Steel-fibre-reinforced concrete panels exposed to air blast loading”, *P. I. Civil Eng.- Str. B.*, **134**(44), 319-331.
- Lu, Y. and Xu, K. (2004), “Modelling of dynamic behaviour of concrete materials under blast loading”, *Int. J. Solids Struct.*, **41**, 131-143.
- Lu, Y. and Wang, Z. (2006), “Characterization of structural effects from above-ground explosion using coupled numerical simulation”, *Comput. Struct.*, **84**, 1729-1742.
- Lubliner, J. (1990), *Plasticity Theory*. USA: McMillan.
- Luccioni, B.M., Ambrosini, D. and Danesi, R. (2004), “Analysis of building collapse under blast loads”, *Eng. Struct.*, **26**, 63-71.
- Luccioni, B., Ambrosini, D. and Danesi, R. (2005), “Predicting the location and size of an explosive device detonated in an urban environment using evidence from building damage”, *P. I. Civil Eng.- Str. B.*, **158**, 1-12.
- Luccioni, B., Ambrosini, D. and Danesi, R. (2006), “Blast load assessment using hydrocodes”, *Eng. Struct.*, **28**(12), 1736-1744.
- Luccioni, B. and Luege, M. (2006), “Concrete pavement slab under blast loads”, *Int. J. Impact Eng.*, **32**(8), 1248-1266.
- Malvar, L.J., Crawford, J.E., Wesevich, J.W. and Simons, D. (1997), “A plasticity concrete material model for DYNA3D”, *Int. J. Impact Eng.*, **19**(9-10), 847-873.
- Mays, G.C., Hetherington, J.G. and Rose, T.A. (1999), “Response to blast loading of concrete wall panels with openings”, *J. Struct. Eng.*, ASCE, **125**(12), 1448-1450.
- Meel, A., O’Neill, L.M., Levin, J.H., Seider, W.D., Oktem, U. and Keren, N. (2007), “Operational risk assessment of chemical industries by exploiting accident databases”, *J. Loss Prevent. Proc.*, **20**, 113-127.
- Millington G.S. (1994), “Discussion of ‘The protection of buildings against terrorism and disorder’ by C. L. Elliott, G. C. Mays and P. D. Smith”, *P. I. Civil Eng.- Str. B.*, **104**, 343-346.

- Park, K., Mannan, M.S., Jo, Y., Kim, J., Keren, N. and Wang, Y. (2006), "Incident analysis of Bucheon LPG filling station pool fire and BLEVE", *J. Hazardous Mater.*, **A137**, 62-67.
- Perry, R.H. and Green, D. (1984), *Perry's Chemical Engineers' Handbook*. 6th New York, McGraw-Hill.
- Planas-Cuchi, E., Salla, J.M. and Casal, J. (2004), "Calculating overpressure from BLEVE explosions", *J. Loss Prevent. Proc.*, **17**, 431-436.
- Planas-Cuchi, E., Gasulla, N., Ventosa, A. and Casal, J. (2004b), "Explosion of a road tanker containing liquified natural gas", *J. Loss Prevent. Proc.*, **17**, 315-321.
- Razus, D.M. and Krause, U. (2001), "Comparison of empirical and semi-empirical calculation methods for venting of gas explosions", *Fire Safety J.*, **36**, 1-23.
- Sercombe, J., Ulm, F. and Toutlemonde, J. (1998), "Viscous hardening plasticity for concrete in high rate dynamics", *J. Eng. Mech.*, ASCE, **124**(9), 1050-1057.
- Smith, P.D. and Hetherington, J.G. (1994), *Blast and ballistic loading of structures*. Great Britain: Butterworth-Heinemann Ltd.
- Stawczyk, J. (2003), "Experimental evaluation of LPG tank explosion hazards", *J. Hazardous Mater.*, **B96**, 189-200.
- Tekalur, S.A., Shivakumar, K. and Shukla, A. (2008), "Mechanical behavior and damage evolution in E-glass vinyl ester and carbon composites subjected to static and blast loads", *Composites: Part B*, **39**, 57-65.
- TNO CPR 14E (Yellow Book) (2005), *Methods for the Calculation of physical Effects Due to the Release of Hazardous Materials (liquids and gases)*. Editors: C.J.H. van den Bosch, R.A.P.M. Weterings. Voorburg, Netherlands Committee for the Prevention of Disasters., 3rd ed., 2nd revised print.
- U.S. Chemical Safety and Hazard Investigation Board (2007), *Investigation Report. Refinery Explosion and Fire (15 Killed, 180 Injured)*. Report No. 2005-04-I-TX. March.
- van den Berg A.C., van der Voort, M.M., Weerheijm, J. and Versloot, N.H.A. (2004), "Expansion-controlled evaporation: A safe approach to BLEVE blast", *J. Loss Prevent. Proc.*, **17**, 397-405.
- Wu, C., Hao, H. and Lu, Y. (2005), "Dynamic response and damage analysis of masonry structures and masonry infilled RC frames to blast ground motion", *Eng. Struct.*, **27**, 323-333.
- Yi, P. (1991), *Explosionseinwirkungen auf Stahlbetonplatten*. Zur Erlangung des akademischen Grades eines Doktor-Ingenieurs der Fakultät für Bauingenieur- und Vermessungswesen der Universität Fridericiana zu Karlsruhe (TH).
- Zheng, S., Haussler-Combe, U. and Eibl, J. (1999) "New approach to strain rate sensitivity of concrete in compression", *J. Eng. Mech.*, ASCE, **125**(12), 1403-1410.